FATIGUE CRACK CLOSURE IN AL-LI 2090 ALLOY

H. Y. JUNG* and S. D. ANTOLOVICH**
*Department of Civil and Environmental Engineering, Jeonju University,
Jeonju, 560-759, South Korea
**School of Mechanical and Material Engineering, Washington State University,
Pullman, WA, 99164 , USA

ABSTRACT

Fatigue crack propagation testing of Al-Li 2090 alloy specimen was performed to investigate fatigue crack closure in terms of crack length. A simple analytical model that is analogous to the experimental procedure for determining crack closure load has been developed to predict variations of closure stress intensity factors as a function of crack length. From the analysis, the variation of closure stress intensity factors was shown to be directly correlated to the roughness (i.e., the asperity geometry and distribution) of the crack surfaces. When the asperity height is relatively high as compared to the crack length, the closure stress intensity factors become a function of the crack length. Otherwise, the closure stress intensity factors appear to be essentially independent of the crack length. Also, an efficient method for estimating the experimental closure load and stress intensity factor has been developed using crack surface opening displacements at the load line. The resulting data appeared to correlate very well with analytical results.

KEYWORDS

Fatigue crack closure, aluminum-lithium, surface roughness, closure stress intensity factor

INTRODUCTION

Much experimental work investigating the relations between the roughness dimension and crack closure measurements has appeared in the literature (Allison and Williams, 1985; Liaw et al., 1987; Zawada and Nicholas, 1988). Most attention was focused on the effects of microstructure (e.g., grain size) on crack closure level in the near-threshold regime. In some of the work, the importance of slip character on closure at relatively high levels of ΔK has been emphasized (Allison, 1988; Bretz et al., 1984). For example, in some materials such as Ti-8Al or ferrous alloys, crack closure was seen over a broad ΔK range (including relatively high crack growth rates) and it was found that the magnitude of the roughness dimension on the crack surface can play an important role in crack closure behavior with increasing crack growth. From the experimental data, it was shown that the closure stress intensity factors for most titanium alloys are constant regardless of the amount of crack growth, but for some ferrous alloys they decrease in a reversed-exponential manner as the crack length increases. In this study, a model predicting both variations will be developed on the basis of Linear Elastic Fracture Mechanics (LEFM) concepts. To find the effects of

roughness dimension on the crack closure level, an analytical simulation of the experimental procedure is introduced. In addition, a review of experimental procedures used in determining closure load by the extrapolation of two compliance curves will be made and a method of eliminating the disadvantages of such techniques will be suggested.

EXPERIMENTAL PROCEDURE

The material studied was as-received Al-Li 2090 T8E41 alloy. Compact type specimens, 25.4 mm wide, 30.48 mm high, and 2.54 mm thick, were used to measure the fatigue crack propagation (FCP) rates in accord with ASTM-E647. All specimens were side-grooved to a depth of 0.127 mm to restrict crack propagation in the L-T orientation. The thickness on the net section was used for calculating stress intensity factors. Fatigue crack propagation tests were conducted using a digitally-controlled closed-loop servo-hydraulic machine under ambient laboratory conditions. Two different load ratios($R=P_{min}/P_{max}$), 0.1 and 0.7, were chosen to study crack closure and roughness dimension. The loading frequency was 5 Hz with a haversine waveform. Various load ranges of 356 ~ 761 N were used for increasing ΔK tests. The crack length was determined by three different methods: the standard potential drop method using a constant DC input of 10 amps; the compliance technique; and optically using a travelling microscope. A laser extensometer having a maximum resolution of 10^{-7} mm was used to measure the distance between the notch edges at the load line.

ANALYTICAL MODEL

Experimentally, the closure load, P_{cl}, is determined by extrapolating two segments of compliance curves and finding the intersection as shown in Fig. 1(a). This procedure is based on the physical notion that contact occurs when two straight lines intersect, indicative of a change in the compliance of the cracked body. However, this procedure significantly simplifies the actual process of crack surface contact, since some contact already occurred at P_1 before the load reaches P_{cl}. In this case, the contact stress distributions on the contact area may be expressed by the assumed function:

$$p(x) = p_0 (1-x/c)^n \qquad (1)$$

The schematic views of this and its parameters are shown in Figure 1(b). If the distributed contacts shown in Fig. 1(b) are converted to contact by a single equivalent imaginary rigid asperity, the asperity height corresponds physically to the crack surface opening displacement (COD) occurring at the location of the single asperity, C_{cl}, resulting from an equivalent concentrated force. For an assumed value of n, the asperity location in the equivalent system can be analytically found by invoking the following assumed constraints:

a) the total contact force summed up along the crack surface is equal to the concentrated force in the equivalent system and

b) both the distributed forces along the crack surface and the equivalent concentrated force develop the same crack surface opening displacement at the location of C_{cl}.

The concept describes the fact that if the equivalent force is located at C_{cl}, both systems are equivalent. In Ref. (Jung, 1994), C_{cl} is found for cases of crack closure in the center cracked tensile (CCT) specimen and the compact tension (CT) specimen and various values of n.

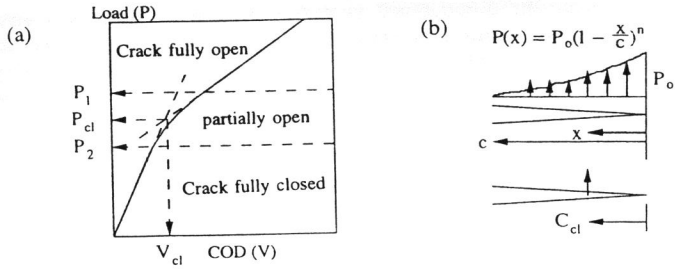

Fig. 1. (a) Determination of closure load and closure crack opening displacement. (b) Closure stress distribution in the wake zone behind crack tip and equivalent system.

To obtain the variation of closure stress intensity factor with crack extension, two crack configurations having crack lengths of $a^{(1)}$ and $a^{(2)}$, respectively, are considered as shown in Fig. 2. $a^{(1)}$ is the crack length obtained after precracking or the crack length at which the measurements of crack closure are made for the first time. It is assumed that an asperity lying between two fracture surfaces is initially 2D units high and it is located at a distance of $C_{cl}^{(1)}$ from the crack tip. $C_{cl}^{(1)}$ is expressed as $c_0 a^{(1)}$, where c_0 is a constant which can be determined through analysis using experimental data. $a^{(2)}$ is the crack length increased by an incremental change in crack length from $a^{(1)}$. Regarding the change in crack length, the ratio between two crack lengths, R_0, is defined as:

$$R_0 = a^{(2)}/a^{(1)} = (a^{(1)} + \Delta a)/a^{(1)} \qquad (2)$$

Also, an asperity is assumed to have a height of $(2D)\gamma$. The constant, γ, accounts for changes in the asperity height resulting from changes in crack tip deformation and the roughness of the crack surface with crack growth. As a crack grows, the plastic zone size and the magnitude of plastic strain increase. Thus the resulting change in crack tip deformation and roughness on crack surface will be a function of crack length. The asperity is also assumed to be located at the distance of $C_{cl}^{(2)}$ from the crack tip, which is defined as a new contact distance for the growing crack. For simplicity, $C_{cl}^{(2)}$ is considered for two different cases; one is that $C_{cl}^{(2)}$ is assumed to be $R_0 C_{cl}^{(1)}$ (Model A) and the other is that $C_{cl}^{(2)}$ is assumed to be independent of the increase in crack length (Model B).

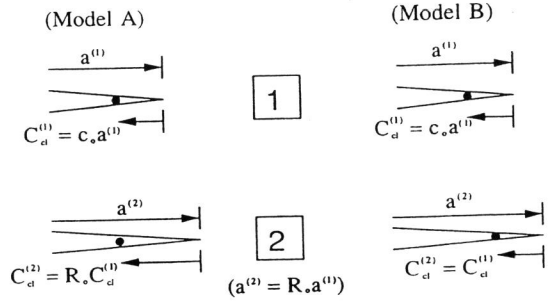

Fig. 2. Schematic view of models used to predict variations of closure load with crack growth.

Now, in order to simulate the experimental procedure by a single asperity contact, an asperity in both crack configurations is assumed to come into contact between the fracture surfaces for remote loads, $P_{cl}^{(1)}$ and $P_{cl}^{(2)}$, respectively. Then, for a given geometry and asperity dimension in each configuration, the crack surface opening displacement resulting from a remote equivalent load must be equal to the height of the asperity to have the asperity contact. This results in the following equations:

$$P_{cl}^{(1)} F'(a^{(1)}, x=a^{(1)}-C_{cl}^{(1)}) = 2D \tag{3}$$

$$P_{cl}^{(2)} F'(a^{(2)}, x=a^{(2)}-C_{cl}^{(2)}) = (2D)\gamma \tag{4}$$

where F'(a,x) is the shape function for the crack surface opening displacement calculated for the remote equivalent load and it is expressed as:

$$F'(a,x) = Y F(a,x) \alpha_R(a) \tag{5}$$

Here Y is a material constant and F(a,x) and $\alpha_R(a)$ are the shape function and geometric function for finite dimensions, respectively. From Eqs. (3) and (4) the closure load, $P_{cl}^{(2)}$, for the increased crack length is found as:

$$P_{cl}^{(2)} = (\gamma/R) P_{cl}^{(1)} \tag{6}$$

where

$$R = F'(a^{(2)}, x=a^{(2)}-C_{cl}^{(2)})/F'(a^{(1)}, x=a^{(1)}-C_{cl}^{(1)}) \tag{7}$$

Using $P_{cl}^{(2)}$, the closure stress intensity factor for the increased crack length is calculated by:

$$K_{cl}^{(2)} = P_{cl}^{(2)} U(a^{(2)}) \tag{8}$$

where U(a) is the weight function used to calculate the stress intensity factor. By manipulating Eqs. (6) and (8) and noting that

$$P_{cl}^{(1)} = K_{cl}^{(1)}/U(a^{(1)}) \tag{9}$$

the following is obtained:

$$K_{cl}^{(2)} = (\gamma/R) (U(a^{(2)})/U(a^{(1)})) K_{cl}^{(1)} \tag{10}$$

Therefore, the variation of closure stress intensity factor with crack growth can be found in normalized form using the initially measured value in terms of crack length and some assumptions for the constants. The expressions for closure load and stress intensity factor for both Models A and B and the geometry of the CCT or CT specimens are detailed in Ref. (Jung, 1994).

In some cases, the change in the asperity dimension can be obtained by measuring the crack surface opening displacement at the load line normal to the crack growth direction when

asperity contact occurs. This quantity is V_{cl} in Fig. 1(a), which corresponds to the crack closure load, P_{cl}. The V_{cl}'s for two crack configurations are defined, respectively, as:

$$V_{cl}^{(1)} = P_{cl}^{(1)} F'(a^{(1)}, x=0) \tag{11}$$

$$V_{cl}^{(2)} = P_{cl}^{(2)} F'(a^{(2)}, x=0) \tag{12}$$

From Eqs. (11) and (12), a closure ratio is given by:

$$V_{cl}^{(2)}/V_{cl}^{(1)} = (P_{cl}^{(2)}/P_{cl}^{(1)}) F'(a^{(2)}, x=0)/F'(a^{(1)}, x=0) \tag{13}$$

Substituting Eq. (6) into Eq. (13) yields:

$$V_{cl}^{(2)}/V_{cl}^{(1)} = (\gamma/R) F'(a^{(2)}, x=0)/F'(a^{(1)}, x=0) \tag{14}$$

Therefore, the variation of asperity height is expressed as:

$$\gamma = (V_{cl}^{(2)}/V_{cl}^{(1)}) R F'(a^{(1)}, x=0)/F'(a^{(2)}, x=0) \tag{15}$$

Here, R was given in Eq. (7), which depends on the asperity location. In some cases such as Model A in the CCT specimen, when the function for crack surface opening displacement varies linearly with crack length and asperity location, γ is simply given by:

$$\gamma = V_{cl}^{(2)}/V_{cl}^{(1)} \tag{16}$$

Therefore, the change of asperity height can be measured directly at the load line. In other cases, it becomes a function of asperity location, so that the measurements of γ are subjected to constraints for the assumed value of n. Using this concept, the crack closure load and stress intensity factor are determined, respectively, as:

$$P_{cl}^{(2)} = (V_{cl}^{(2)}/V_{cl}^{(1)}) (F'(a^{(1)}, x=0)/F'(a^{(2)}, x=0)) P_{cl}^{(1)} \tag{17}$$

$$K_{cl}^{(2)} = (V_{cl}^{(2)} F'(a^{(1)}, x=0) U(a^{(2)})/V_{cl}^{(1)} F'(a^{(2)}, x=0) U(a^{(1)})) K_{cl}^{(1)} \tag{18}$$

Note that the asperity is assumed to be extremely rigid.

RESULTS AND DISCUSSION

In order to see the differences between Models A and B, the crack closure load and corresponding closure stress intensity factor as a function of crack length are plotted as shown in Figs. 3(a) and 3(b). For simplicity, they are calculated for a constant asperity height and for $0.25 \le a/W \le 0.7$ and a constant applied load. The resulting variations are expressed in normalized form by dividing by the starting values, i.e., $P_{cl}(1)$ and $K_{cl}(1)$, respectively. In a increasing ΔK tesing with a constant load, the maximum stress intensity factors are only a function of crack length. These are also normalized by the starting value

($K_{max}(1)$). Figure 3(a) shows a monotonically decreasing crack closure load for both models. But the crack closure load for Model A decreases more rapidly than the one for Model B as a crack grows. In Fig. 3(b), variations of closure stress intensity factors with crack growth are shown. It decreases monotonically for Model A, but for Model B it is almost constant with increasing crack length. The curves in Fig. 3(b) are very similar to the schematic variations of closure stress intensity factors for roughness-induced crack closure in Ref. (Allison, 1988), which was experimentally measured for several materials. The only difference is that Model A predicts an exponentially decreasing value with crack extension. The differences between Models A and B may be explained on a physical basis in terms of the roughness dimension on the fracture surface. If the roughness dimension is small compared to the crack length, it is not comparable to the crack surface opening displacement, so that C_{cl} seems not to vary much as a crack grows. In other words, a few leading asperities near the crack tip are the most effective ones for crack closure. In this case, the closure stress intensity factor will become constant with crack extension corresponding to Model B. On the other hand, if the roughness is large, it becomes comparable to the crack surface opening displacement and it is expected that there are more chances of contact for distant asperities and the contact areas increase with crack growth. Then, C_{cl} increases as the crack length increases, so that variations of closure stress intensity factor can be understood in terms of Model A. From this, it is seen that this model can lead to different variations of K_{cl} for different levels of the roughness dimension. Actually, in experiments, it was found that the average roughness dimension for Model B (Drury, 1992) is much smaller ($\sim 10\mu m$) than the one ($\sim 300\mu m$) for Model A (Jung and Antolovich, 1995). Also, the contact ranges observed from experiments are different for both cases, i.e., contact for Model B occurs only near the crack tip (within 50 microns) but it could occur all over the crack surfaces for Model A. Here, the materials considered for Models A and B are Al-Li 2090 and IN-718, respectively.

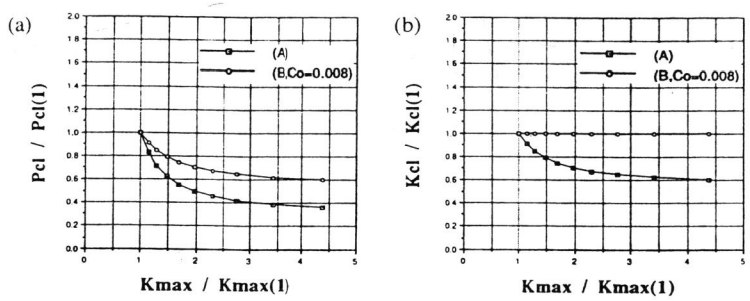

Fig. 3. Variations of normalized (a) P_{cl} and (b) K_{cl} with crack growth for Models A and B.

The analytical model (Model A) is examined with respect to variations of closure stress intensity factor with crack growth through comparisons with experimental data for Al-Li 2090 Alloy. From the load-displacement curves measured as a function of crack length, the crack closure loads are found using extrapolation techniques for the two compliance curves. They are plotted as Exp.(P_{cl}) in Fig. 4(a). Also, the resulting closure stress intensity factors are plotted as Exp.(K_{cl}) in Fig. 4(b). From these figures their variation in the early stages of crack growth is unpredictable due to scatter in the data. In order to eliminate this problem, Eqs. (17) and (18) for obtaining crack closure load and stress intensity factor are

used. The experimental parameter in the equations, which is the variation of closure crack surface opening displacement at the load line (V_{cl}), is measured as shown in Fig. 5. The crack surface opening displacements at the load line for the maximum and minimum load, i.e., V_{max} and V_{min}, increase as the crack length increases, as expected. However, the closure crack surface opening displacement at contact, which was defined in Fig. 1(a), is nearly constant as a function of crack length. Therefore, the resulting crack closure load and stress intensity factor as a function of crack length are plotted as curves of $P_{cl}(V_{cl})$ and $K_{cl}(V_{cl})$ in Figs. 4(a) and 4(b), respectively. Comparing both experimental curves, it is found that the trends are the same if the data for experimentally determined P_{cl} and K_{cl} are simply shifted to the left. The analytical solutions for Model A and the CT specimen are used to calculate variations of closure load and stress intensity factor for various assumed c_0's. From Figs. 4(a) and 4(b), it is found that for $c_0 \approx 0.4$ both analytical and experimental data are correlated. As mentioned in the previous section, in order for the analytical curves to yield an acceptable fit of the experimental data, the parameter c_0, which was given as a material constant, must be appropriately assumed or experimentally determined. From the literature (Hu et al., 1991), it was experimentally seen that "duplex ceramic" materials show the same $c_0 \approx 0.4$ (n=0.7) and the extensive contact process zone. This also was seen in Al-Li 2090 Alloy, in which the contact occurs over a large area of the fracture surfaces due to the large roughness dimension.

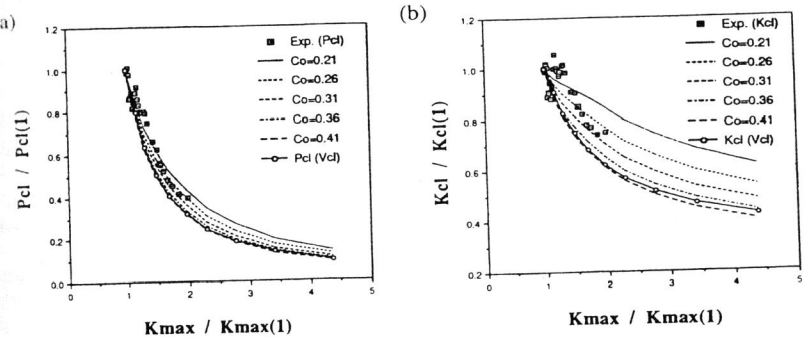

Fig. 4. Comparisons of (a) Exp.(P_{cl}) and $P_{cl}(V_{cl})$ and (b) Exp.(K_{cl}) and $K_{cl}(V_{cl})$ with analytical results for various c_0's.

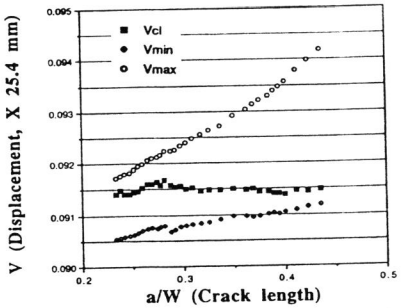

Fig. 5. Variations of crack surface opening displacement at the load line with crack growth for typical P_{max}, P_{min}, and P_{cl} in Al-Li 2090 Alloy.

CONCLUSIONS

A simple analytical model that corresponds to the experimental procedure for determining crack closure load has been developed to predict variations of closure stress intensity factors as a function of crack growth. From the analysis, the variation of closure stress intensity factors was shown to be directly correlated to the roughness dimension (or asperity height) on crack surfaces. When the asperity height is assumed to be relatively high compared to the crack length, the closure stress intensity factors become a function of the crack length. But if this is not the case, the closure stress intensity factors appear to be essentially independent of the crack length. Also, an efficient method for estimating the experimental closure load and stress intensity factor has been developed. The resulting data appeared to correlate very well with analytical results. From these approaches it was demonstrated that the closure stress intensity factors decrease monotonically rather than in a reversed-exponential manner as the crack length increases.

ACKNOWLEDGEMENTS

This work was funded through the Office of Naval Research, Grant No. N0014-89J-1708. Helpful discussions with Dr. G.R. Yoder, the grant monitor, are greatfully acknowledged.

REFERENCES

Allison, J. E. (1988). The measurement of crack closure. In: *Fracture Mechanics: Eighteenth Symposium* (D.T. Read and R.P. Reed, Eds.), ASTM STP 945, pp. 913-933. ASTM, Philadelphia, PA.

Allison, J. E. and J. C. Williams (1985). The role of crack closure. In: *Titanium, Science and Technology* (G. Luetjering, U. Zwicher, and W. Bunk, Eds.), vol. 4, pp. 2243-2250. DGM Publications, Oberursel, West Germany.

Bretz, P. E., J. I. Petit, and A. K. Vasudevan (1984). The effects of grain size. In: *Fatigue Crack Growth Threshold Concepts* (D. Davidson, and S. Suresh, Eds.), pp. 163-183, Warrendale, PA.

Drury, W. (1992). Development of quantitative fractography. Ph.D. dissertation, Georgia Institute of Technology, Atlanta, GA.

Jung, H. Y. (1994). Characterization of fatigue crack closure. Ph.D. dissertation, Georgia Institute of Technology, Atlanta, GA.

Jung, H. Y. and S. D. Antolovich (1995). Experimental characterization of roughness. *Scripta Metall. et. Mat.*, **33**, 275-281.

Hu, X. Z., E. H. Lutz, and M. V. Swain (1991). Crack-tip-bridging stresses. *J. Am. Ceram. Soc.*, **74**, 1828-32.

Liaw, P. K., T. R. Leax, T. R. Fabis, and J. K. Donald (1987). Fatigue crack growth. *Eng. Fract. Mech.*, **26**, 1-13.

Zawada, L. and T. Nicholas (1988). The effect of Loading history. In: *Fracture Mechanics: Eighteenth Symposium* (D.T. Read and R.P. Reed, Eds.), ASTM STP 945, pp. 193-205. ASTM, Philadelphia, PA.